

Energy partition between splitting fission fragments

H.Y. Shang,¹ Y. Qiang,¹ and J.C. Pei^{1,2,*}

¹State Key Laboratory of Nuclear Physics and Technology,
School of Physics, Peking University, Beijing 100871, China

²Southern Center for Nuclear-Science Theory (SCNT),
Institute of Modern Physics, Chinese Academy of Sciences, Huizhou 516000, China
(Dated: January 14, 2025)

From the microscopic view, the energy partition between two fission fragments are associated with the splitting of wave functions of an entangled fissioning system, in contrast to most fission models using an explicit statistical partition of excitation energies by invoking level densities of fragments. The dynamical fission evolution is described within the time-dependent Hartree-Fock+BCS framework. Excitation energies of isotopic fission fragments are obtained with the particle-number projection method after the dynamical splitting of ^{238}U . The resulting excitation energies of light and heavy fragments illustrate the appearance of sawtooth structures. We find that the pairing strengths have significant influences on the partition of excitation energies. Furthermore, excitation energies of isotopic fragments increase with increasing neutron numbers, suppressing the production of neutron-rich beams in rare-isotope beam facilities.

Introduction.— In the final stage of nuclear fission, the majority of nuclear energy is released through the enormous kinetic energies of splitting fission fragments. However, the remain considerable part of nuclear energy is stored as excitation energies of primary fission fragments. Consequently, the de-excitation fission fragments is realized by neutron emissions, γ radiations, and then β -decays [1]. Therefore, the energy partition between two fragments plays an indispensable role in determining multiple post-fission observables and their correlations.

The excitations of fragments are caused by the dissipative motion and shape distortions. The dissipation can play a significant role even in the final splitting stage [2]. The shape distortion and shell effects of fragments are important in the energy partition [3]. The non-equilibrium non-adiabatic fission dynamics, shell effects, dynamical pairing correlations, shapes of primary fragments, and energy dependencies can be naturally described by the microscopic time-dependent density functional theory (TD-DFT) [2, 4–15]. It has been pointed out that the energy partition is later than particle partition [16]. In previous fission studies of ^{240}Pu , the light fragments acquire more excitation energies than that of heavy fragments [4]. This is consistent with observations that light fragments emit more neutrons compared to heavy fragments from the fission of actinide nuclei. With increasing excitation energies, the difference in excitation energies between light and heavy fragments are reduced [4].

Experimentally, the average number of neutrons, i.e., neutron multiplicities, emitted from fission fragments shows the puzzling sawtooth structures in dependence of fragment masses [17, 18]. This provides a unique chance to understand the energy sharing between two fission fragments. Conventionally the excitation energy sharing

between fission fragments are described as at the statistical equilibrium by invoking the different level densities of fragments [3, 19–22]. It has been pointed out that shape-dependent level densities can better describe the partition of excitation energies [3]. Within this approach, the slopes of the sawtooth structures are slightly underestimated [3]. Usually different temperatures in light and heavy fragments have to be adopted to reproduce neutron multiplicities [20, 21]. The sawtooth structures are also shown in the distributions of neutron excess in dependence of fragment-charge number [23, 24] and angular momentum in dependence of fragment masses [25].

Recently, we proposed that the quantum entanglement is crucial for the appearance of sawtooth structures in the distributions of excitation energies of fragments and subsequently neutron multiplicities [26]. The sharing of particles between two fission fragments obtained by double particle number projection (PNP) shows a considerable spreading width [26, 27]. The associated energy partition due to the superposition of different particle numbers can be obtained by the PNP method [26]. The distribution of fragment yields has been studied by PNP within the framework of time-dependent generator-coordinate-method and TD-DFT [27–29]. The PNP method has also been used to study heavy ion reactions [30, 31]. In most fission models, the quantum correlations or entanglement between two fission fragments have not been taken into account. It is timely to study energy partition between fission fragments considering quantum entanglement between two fission fragments, in which the entanglement is persistent even two fragment are well separated [26].

In this work, we studied the partition of excitation energies of isotopic fission fragments of ^{238}U , which is relevant for the production of radioactive beams from the fission products after prompt neutron evaporations. For example, the medium-mass neutron-rich beams are mainly produced by the fission of ^{238}U in new-generation rare isotope beam facilities such as FRIB [32], RIBF [33] and HIAF [34]. Three new isotopes have been produced

* peij@pku.edu.cn

in fission reactions of ^{238}U beam in the carbon target in newly operated FRIB [32]. Furthermore, the proposal of photo-fission of ^{238}U driven by a high-power e-LINAC with a convertor target is promising to produce neutron-rich beams [35].

Methods— The time-dependent Hartree-Fock+BCS (TD-BCS) approach is used to describe the dynamical fission evolution beyond the saddle point. The TD-BCS equations can be derived by using the BCS basis or canonical basis in the time-dependent Hartree-Fock-Bogoliubov method [36]. In our previous work, TD-BCS has been extended to study fission dynamics of compound nuclei [4]. The initial configuration of the fissioning nucleus is obtained by deformation-constrained Hartree-Fock+BCS calculations. We employed constrained calculations in terms of quadrupole-octupole deformations (β_2, β_3) . The initial deformation is adopted as $(\beta_2, \beta_3)=(2.4, 1.4)$ for the fission evolution. For nuclear interactions, SkM* [37] and UNEDF1 [38] forces have been adopted, which have been widely used for calculations of nuclear fission barriers. The mixing-type pairing interaction [39] is adopted with strengths $V_p=475$ MeV and $V_n=420$ MeV for SkM* force, and $V_p=415$ MeV and $V_n=375$ MeV for UNEDF1 force. The dynamical evolution is performed with the time-dependent Hartree-Fock (TDHF) solver Sky3D [40] with our modifications of TD-BCS. The initial configurations are obtained using the SkyAX solver [41] to interface with Sky3D.

Based on TD-BCS solutions, the particle numbers of fragments and the fissioning nucleus are not well defined. The particle numbers in two fragments are in a superposition state. The double PNP on the total space and a partial space is applied to determine the particle numbers of two complementary fragments.

The double projection operator is written as

$$\hat{P}^q(N_T^q, N_P^q) = \frac{1}{4\pi^2} \iint d\theta_T d\theta_P \quad (1)$$

$$e^{i\theta_T(\hat{N}_T^q - N_T^q)} e^{i\theta_P(\hat{N}_P^q - N_P^q)},$$

where q denotes neutron or proton, T/P denotes the projection on the total space or a partial space and \hat{N}_P^q denotes the particle number operator. Note that the particle number operator is $\hat{N}_P^q = \int d\mathbf{r} \hat{C}^\dagger(\mathbf{r}) \hat{C}(\mathbf{r}) \Theta(\mathbf{r})$, where $\Theta(\mathbf{r})$ is a mask function to obtain an exclusive partial space. The projected states with particle numbers deviating from the average number up to 8 particles are calculated.

The PNP on the wave functions of each fragment leads to a two-dimensional distribution of fragments in terms of (Z, N) , in which the formation probability of each fragment is the expectation value of $\langle \Psi | \hat{P}^n(N_T, N_P) \hat{P}^p(Z_T, Z_P) | \Psi \rangle$. The projected binding energy of each fragment is obtained by

$$E_{\text{proj}} = \frac{\langle \Psi | \hat{H} \hat{P}^n(N_T, N_P) \hat{P}^p(Z_T, Z_P) | \Psi \rangle}{\langle \Psi | \hat{P}^n(N_T, N_P) \hat{P}^p(Z_T, Z_P) | \Psi \rangle}, \quad (2)$$

which is actually calculated as [42, 43]

$$E_{\text{proj}} = \int d\theta_n \int d\theta_p Y_{\theta_n} Y_{\theta_p} \text{Tr} \left\{ t \left(\rho_{\theta_n}^n + \rho_{\theta_p}^p \right) \right. \\ \left. + \frac{1}{2} \left(\Gamma_{\theta_n}^{\text{nn}} \rho_{\theta_n}^n + \Gamma_{\theta_p}^{\text{pp}} \rho_{\theta_p}^p + \Gamma_{\theta_p}^{\text{np}} \rho_{\theta_n}^n + \Gamma_{\theta_n}^{\text{pn}} \rho_{\theta_p}^p \right. \right. \\ \left. \left. - \Delta_{\theta_n}^n \bar{\kappa}_{\theta_n}^{n*} - \Delta_{\theta_p}^p \bar{\kappa}_{\theta_p}^{p*} \right) \right\} \\ Y_{\theta_q} = \langle \Psi | e^{i\theta_T(\hat{N}_T^q - N_T^q)} e^{i\theta_P(\hat{N}_P^q - N_P^q)} | \Psi \rangle / \langle \Psi | \hat{P}^q | \Psi \rangle,$$

where $\rho_\theta, \kappa_\theta$ are transition densities. The excitation energy of each fragment is obtained by the subtraction between the projected binding energy in the splitting process and the ground state energy. This method has been applied to calculate excitation energies of products in multi-nucleon transfer reactions [31]. In practical calculations, a series of transition densities like the current density, spin-orbit density have to be calculated at each θ . The calculations are very costly because the proton-neutron mixing terms involve fourfold integrations. The calculations could be problematic when the denominator in Eq. (2) is tinny, and a cutoff at 5×10^{-4} is applied.

Results.— Firstly the distributions of fission yields of ^{238}U after PNP on the splitting fission event are obtained. Fig.1(a) shows the distributions of projected fission yields as a function of fragment masses, calculated with SkM* and UNEDF1 forces, respectively. It can be seen that the peak is around $A=136$ with SkM* force, but the peak is around $A=138$ with UNEDF1 force. The peak widths are similar and the half-widths are about 8 number of particles. It is known that UNEDF1 results in a slightly lower fission barriers than that of SkM* [38]. This could be a reason that the fission yield peak from UNEDF1 calculations is slightly more asymmetric. Correspondingly, its total kinetic energy (TKE) is smaller with a longer scission neck. The resulting TKE of SkM* calculations is 168.9 MeV while TKE of UNEDF1 calculations is about 159.5 MeV. Note that the average experimental TKE from photofission of ^{238}U is around 170 MeV [44].

Pairing correlations are important in descriptions of fission probabilities [45] and dynamical fission evolutions [4, 10, 46]. To study the role of pairing correlations in dynamical calculations of particle partition between fission fragments, the distributions of fission yields after PNP are displayed with varying pairing strengths, as shown in Fig.1(b). It can be seen that the peak locations are shifted to more asymmetric fission modes with increasing pairing strengths. With TDHF calculations without pairing correlations, the peak location is around $A=132$ and is close to the asymmetric S1 fission channel [47, 48]. This situation is similar to our previous studies of the fission of ^{240}Pu [4]. The peak locations from calculations with pairing strengths reduced by a factor of 0.9 are close to the original results. However, the peak location is shifted to $A=142$ if the pairing strength increased by a factor of 1.2. It has been pointed out that a larger pairing strength results in a longer scission neck [2], which could be related to more asymmetric

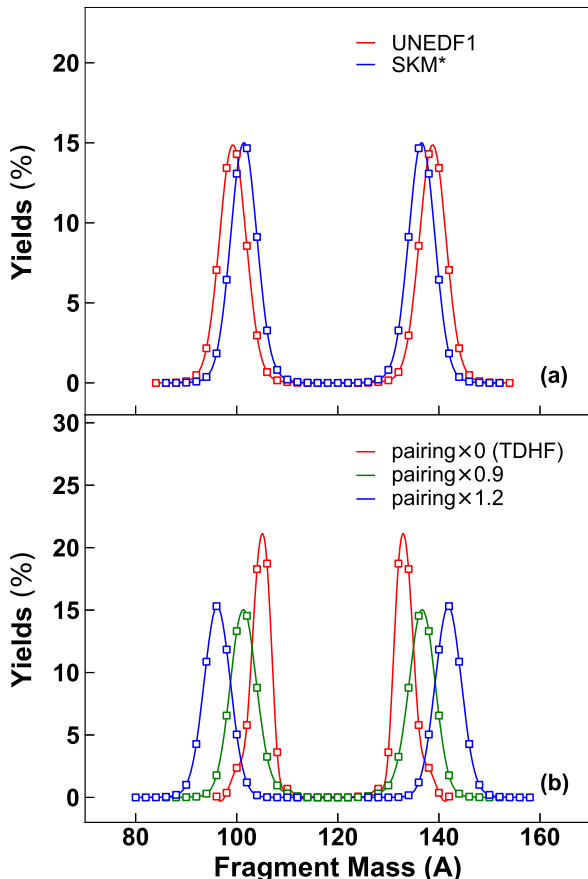


FIG. 1. Fission yields of ^{238}U based on TD-BCS+PNP calculations of the splitting fission fragments. (a) Results obtained with SkM* and UNEDF1 forces, respectively. (b) Results obtained with SkM* force and varying pairing strengths corresponding to factors of 0.0 (TDHF), 0.9 and 1.2, respectively.

fission yields. Within TDHF, the width from PNP is obviously smaller than that of TD-BCS+PNP calculations. This implies that the spreading width of fission yields can be enhanced by including many-body correlations. It is known that the width of S1 channel is indeed narrower than that of S2 channel [47]. With increasing pairing strengths, the scission neck becomes longer and the resulting TKE become smaller. The TKE corresponding to pairing factors of 0.0, 0.9 and 1.2 are 174.2, 169.6 and 160.3 MeV, respectively.

It is known that average excitation energies of fission fragments can be obtained by TD-BCS calculations without PNP. Within TD-BCS, the light fragment has higher excitation energies than that of the heavy fragment at low energy fission [4]. In this work, we are interested to study the distribution of excitation energies of all fission fragments with PNP. This is related to the intriguing sawtooth structures of neutron multiplicities.

Fig.2 shows the resulting excitation energies of different isotopic fragments. It can be seen that UNEDF1 results are similar to that of SkM* results. The results of

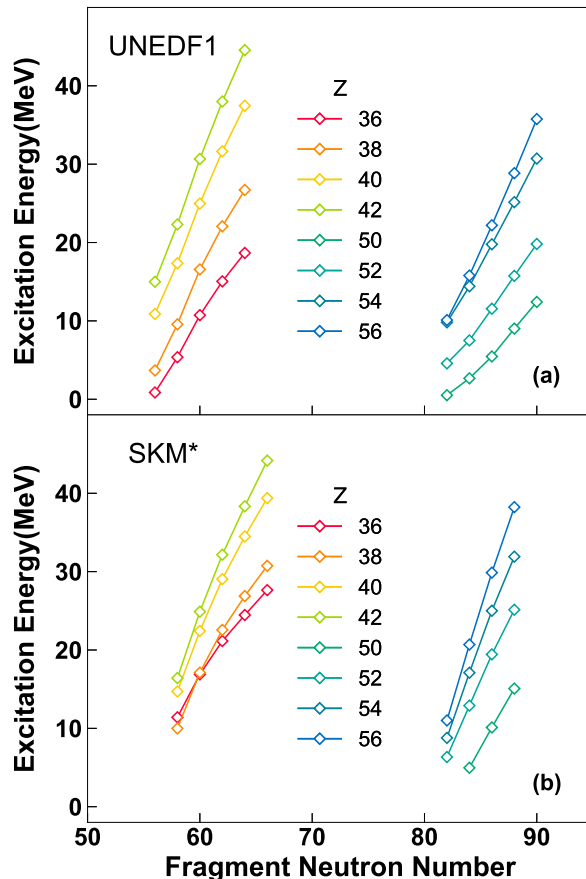


FIG. 2. Excitation energies of isotopic fission fragments of ^{238}U after PNP on the splitting fission fragments. (a) Results obtained with SkM* force; (b) Results obtained with UNEDF1 forces.

isotopes around $Z=46$, i.e., the symmetric fission channel, having very small yields, are not shown. Usually the average neutron multiplicities are illustrated in terms of fragment masses. In our calculations, the detailed results shows that the distributions of excitation energies of isotopic fragments have positive slopes. This actually explains the origin of sawtooth structures. Generally light fragments have higher excitation energies than that of heavy fragments. However, this is not the case for two complementary fragments. For the same isotopic fragments, the heavier fragments have higher excitation energies. It has to be noted that, to obtain realistic two-dimensional distributions of fission yields and excitation energies, fluctuation effects in the fission process should be taken into account, which can significantly alleviate the slopes of sawtooth structures [26].

In Fig.2, excitation energies of isotopic fragments increase as the neutron number increases, which has significant implications. Currently the rare isotope beam facilities [32, 33] mainly rely on the acceleration of fission fragments from ^{238}U . In particular, the Coulomb excitation induced fission of ^{238}U with a high- Z target has ad-

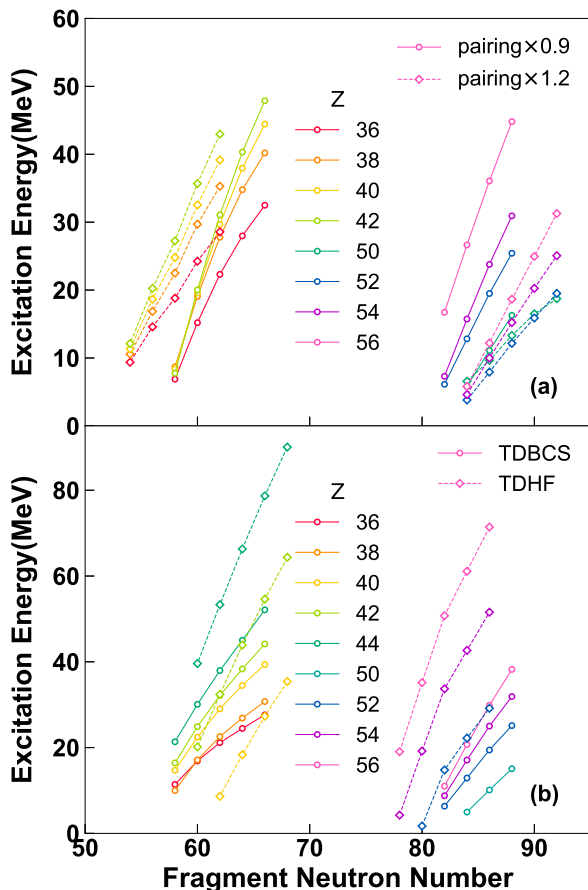


FIG. 3. Excitation energies of isotopic fission fragments from ^{238}U after PNP on the splitting fission fragments. (a) Results obtained with pairing strengths varied by a factor of 0.9 and 1.2 respectively. (b) Results obtained with TDHF (zero pairing) and TD-BCS methods.

vantages for production of neutron-rich beams [49]. The reliable estimation of beam intensities is a practical issue. The beam intensity calculations are conventionally based on the code LISE⁺⁺ [50], which relies on empirical fission yields. It is difficult to simultaneously describe intensities of light and heavy fragments [33]. In our calculations, the heavier isotopes have higher excitation energies, resulting more neutron evaporations. This means that the production of neutron-rich rare isotope beams would be suppressed. The partition of excitation energies would be changed at high energies when sawtooth structures are also washed out [51].

Fig.3 shows the excitation energies of fission fragments with varying pairing strengths. With increasing pairing strengths, the fission yield peaks would be slightly more asymmetric, as shown in Fig.1(b). It can be seen that the maxima excitation energies of fragments are generally reduced with increasing pairing strengths. In particu-

lar, excitation energies of heavy fragments except for the $Z=50$ shell decrease significantly with increasing pairings. In addition, the slopes of excitation energies of light fragments are reduced with increasing pairing strengths. The slopes are overestimated within our approach, which can be alleviated by fluctuation effects [26]. Fig.3(b) shows the excitation energies from TD-BCS+PNP and TDHF+PNP calculations. It can be seen that the excitation energies and its slopes from TDHF+PNP are too large, corresponding to the narrow S1 channel. Our results indicate that many-body correlations in addition to pairing correlations might be useful to obtain reasonable excitation energies of fragments as well as to alleviate the associated slopes. In this respect, fluctuations can be seen as an effective treatment of high-order correlations. Nevertheless, to quantitatively reproduce the distributions of fission yields and neutron multiplicities microscopically is beyond the present work.

Summary.— The excitation energies of isotopic fission fragments from ^{238}U are calculated with the microscopic TD-BCS plus PNP method for deeper understandings of nuclear fission. This is different from most fission models that use the explicit statistical partition of excitation energies between fragments. The dependencies of the energy partition on different Skyrme forces and varying pairing strengths are studied. With increasing pairing strengths, the peak of fission yields shifts to a slightly more asymmetric fission channel. Within TDHF calculations without pairings, the width of fission yields is rather narrow and its peak is close to the S1 fission channel. The obtained excitation energies of isotopic fission fragments explain the origin of sawtooth structures. Furthermore, pairing correlations play a significant role in the partition of energies between fragments. The slope of excitation energies of light fragments would decrease with increasing pairing strengths. For heavy fragments, the excitation energies of heavy fragments except for the $Z=50$ shell would decrease significantly with increasing pairing correlations. The excitation energies based on TDHF+PNP are too large and the associated slopes are very steep. Our results indicate that many-body correlations or fluctuations are essential to obtain reasonable excitation energies. It has to be pointed out that the excitation energy partition and consequently neutron evaporations have practical implications to estimate beam intensities in rare-isotope beam facilities.

ACKNOWLEDGMENTS

This work was supported by the National Key R&D Program of China (Grant No.2023YFA1606403, 2023YFE0101500), the National Natural Science Foundation of China under Grants No.12475118, 12335007. We also acknowledge the funding support from the State Key Laboratory of Nuclear Physics and Technology, Peking University (No. NPT2023ZX01).

-
- [1] M. Bender *et al.*, Future of nuclear fission theory, *J. Phys. G* 47, 113002(2020).
- [2] Y. Qiang and J. C. Pei, Energy and pairing dependence of dissipation in real-time fission dynamics, *Phys. Rev. C* 104, 054604(2021).
- [3] M. Albertsson, B.G. Carlsson, T. Døssing, P. Möller, J. Randrup, S. Åberg, Excitation energy partition in fission, *Phys. Lett. B* 803, 135276(2020).
- [4] Y. Qiang, J. C. Pei, and P. D. Stevenson, Fission dynamics of compound nuclei: Pairing versus fluctuations, *Phys. Rev. C* 103, L031304(2021).
- [5] S. E. Koonin and J. R. Nix, Microscopic calculation of nuclear dissipation, *Phys. Rev. C* 13, 209(1976).
- [6] J. W. Negele, S. E. Koonin, P. Moller, J. R. Nix, and A. J. Sierk, Dynamics of induced fission, *Phys. Rev. C* 17, 1098(1978).
- [7] T. Nakatsukasa, K. Matsuyanagi, M. Matsuo, and K. Yabana, Time-dependent density-functional description of nuclear dynamics, *Rev. Mod. Phys.* 88, 045004(2016).
- [8] P. Goddard, P. Stevenson, and A. Rios, Fission dynamics within time-dependent Hartree-Fock: Deformation-induced fission, *Phys. Rev. C* 92, 054610(2015).
- [9] C. Simenel, K. Godbey, and A. S. Umar, Timescales of Quantum Equilibration, Dissipation and Fluctuation in Nuclear Collisions, *Phys. Rev. Lett.* 124 212504 (2020)
- [10] A. Bulgac, P. Magierski, K. J. Roche, and I. Stetcu, Induced Fission of ^{240}Pu within a Real-Time Microscopic Framework, *Phys. Rev. Lett.* 116, 122504(2016).
- [11] A. Bulgac, S. Jin, K. J. Roche, N. Schunck, and I. Stetcu, Fission dynamics of ^{240}Pu from saddle to scission and beyond, *Phys. Rev. C* 100, 034615(2019).
- [12] G. Scamps, C. Simenel, Impact of pear-shaped fission fragments on mass-asymmetric fission in actinides, *Nature* 564, 382(2018).
- [13] C. Simenel and A. S. Umar, Formation and dynamics of fission fragments, *Phys. Rev. C* 89, 031601(R)(2014).
- [14] Y. Tanimura, D. Lacroix, S. Ayik, Microscopic Phase-Space Exploration Modeling of ^{258}Fm Spontaneous Fission, *Phys. Rev. Lett.* 118, 152501(2017).
- [15] Yue Shi, N. Hinohara, and B. Schuetrumpf, Implementation of nuclear time-dependent density-functional theory and its application to the nuclear isovector electric dipole resonance, *Phys. Rev. C* 102, 044325(2020).
- [16] A. Bulgac, Fission-fragment excitation energy sharing beyond scission, *Phys. Rev. C* 102, 044609 (2020).
- [17] C. Budtz-Jørgensen and H.-H. Knitter, Simultaneous investigation of fission fragments and neutrons in $^{252}\text{Cf(sf)}$, *Nucl. Phys. A* 490, 307(1988).
- [18] K. Nishio, Y. Nakagome, H. Yamamoto, and I. Kimura, Multiplicity and energy of neutrons from $^{235}\text{U}(n_{th},f)$ fission fragments, *Nucl. Phys. A* 632, 540(1998).
- [19] Karl-Heinz Schmidt and Beatriz Jurado, Final excitation energy of fission fragments, *Phys. Rev. C* 83, 061601(R) (2011)
- [20] Y.J.Chen, J. Qian, T.J. Liu, Z.X.Li, X.Z. Wu, and N.C. Shu, Energy partition in ^{235}U fission reaction induced by thermal neutron, *Int. J. Mod. Phys. E* 21, 1250073 (2012)
- [21] K.Fujio, S.Okumura, C. Ishizuka, S. Chiba and T. Katabuchi, Connection of four-dimensional Langevin model and Hauser-Feshbach theory to describe statistical decay of fission fragments, *J. Nucl. Sci. Tech.* 61:1, 84(2024).
- [22] C. Morariu, A. Tudora, F-J. Hamsch, S. Oberstedt and C. Manaiescu, Modelling of the total excitation energy partition including fragment deformation and excitation energies at scission, *J. Phys. G* 39 055103(2012).
- [23] D. Ramos *et al.*, Insight into excitation energy and structure effects in fission from isotopic information in fission yields, *Phys. Rev. C* 99, 024615(2019).
- [24] J.N. Wilson *et al.*, Anomalies in the Charge Yields of Fission Fragments from the $^{238}\text{U}(n,f)$ Reaction, *Phys. Rev. Lett.* 118, 222501(2017).
- [25] J. N. Wilson *et al.*, Angular momentum generation in nuclear fission, *Nature (London)* 590, 566(2021).
- [26] Y. Qiang, J.C. Pei, K. Godbey, Quantum Entanglement in Nuclear Fission, arXiv:2408.07375, *Phys. Lett. B* (accepted), 2025.
- [27] M. Verriere, N. Schunck, and T. Kawano, Number of particles in fission fragments, *Phys. Rev. C* 100, 024612(2019).
- [28] M. Verriere, N. Schunck, and D. Regnier, Microscopic calculation of fission product yields with particle-number projection, *Phys. Rev. C* 103, 054602(2021).
- [29] A. Bulgac, Projection of good quantum numbers for reaction fragments, *Phys. Rev. C* 100, 034612(2019).
- [30] K. Godbey, C. Simenel, and A. S. Umar, Microscopic predictions for the production of neutron-rich nuclei in the reaction $^{176}\text{Yb} + ^{176}\text{Yb}$, *Phys. Rev. C* 101, 034602 (2020)
- [31] K. Sekizawa and K. Yabana, Particle-number projection method in time-dependent Hartree-Fock theory: Properties of reaction products, *Phys. Rev. C* 90, 064614(2014).
- [32] P.N. Ostroumov, O.B. Tarasov, N. Bultman, F. Casagrande, Y. Choi, S. Cogan, M. Cortesi, K. Fukushima, A. Gonzalez et al., Acceleration of uranium beam to record power of 10.4 kW and observation of new isotopes at Facility for Rare Isotope Beams, *Phys. Rev. Accel. Beams* 27, 060101(2024).
- [33] Y. Shimizu, T. Kubo, N. Fukuda, N. Inabe, D. Kameda, H. Sato, H. Suzuki, H. Takeda, K. Yoshida, G. Lorusso, H. Watanabe, et al., Observation of New Neutron-rich Isotopes among Fission Fragments from In-flight Fission of 345 MeV/nucleon ^{238}U : Search for New Isotopes Conducted Concurrently with Decay Measurement Campaigns, *J. Phys. Soc. Jpn.* 87, 014203 (2018).
- [34] X.H. Zhou, J.C. Yang, et al., Status of the high-intensity heavy-ion accelerator facility in China, *AAPPS Bull.* 32, 35 (2022).
- [35] ISAC and ARIEL: The TRIUMF Radioactive Beam Facilities and the Scientific Program, Edited by J. Dilling, R. Krücken, and L. Merminga, Published by Springer, 2014.
- [36] S. Ebata, T. Nakatsukasa, T. Inakura, K. Yoshida, Y. Hashimoto, and K. Yabana, Canonical-basis time-dependent Hartree-Fock-Bogoliubov theory and linear-response calculations, *Phys. Rev. C* 82, 034306(2010).
- [37] J. Bartel, P. Quentin, M. Brack, C. Guet, and H. B. Håkansson, Towards a better parametrisation of Skyrme-like effective forces: A Critical study of the SkM force, *Nucl. Phys. A* 386, 79(1982).
- [38] M. Kortelainen, J. McDonnell, W. Nazarewicz, P.-G. Reinhard, J. Sarich, N. Schunck, M. V. Stoitsov, and

- S. M. Wild, Nuclear energy density optimization: Large deformations, *Phys. Rev. C* 85, 024304 (2012).
- [39] J. Dobaczewski, W. Nazarewicz, and M.V. Stoitsov, Nuclear ground-state properties from mean-field calculations, *Eur. Phys. J. A* 15, 21(2002).
- [40] J. A. Maruhn, P.-G. Reinhard, P. D. Stevenson, and A. S. Umar, The TDHF code Sky3D, *Comp. Phys. Comm.* 185, 2195(2014).
- [41] P.-G. Reinhard, B. Schuetrumpf, and J. Maruhn, The Axial Hartree-Fock+ BCS Code SkyAx, *Comput. Phys. Commun.* 258, 107603 (2021).
- [42] M. Anguiano, J. Egido, and L. Robledo, Particle number projection with effective forces, *Nucl. Phys. A* 696, 467(2001).
- [43] J. A. Sheikh, J. Dobaczewski, P. Ring, L. M. Robledo, and C. Yannouleas, Symmetry restoration in mean-field approaches, *J. Phys. G* 48, 123001(2021).
- [44] A. Göök et al. Fragment characteristics from fission of ^{238}U and ^{234}U induced by 6.5-9.0 MeV bremsstrahlung, *Nuclear Physics A* 851, 1 (2011).
- [45] J. Sadhukhan, J. Dobaczewski, W. Nazarewicz, J. A. Sheikh, and A. Baran, Pairing-induced speedup of nuclear spontaneous fission, *Phys. Rev. C* 90, 061304(R) (2014).
- [46] X. B. Wang, Yongjing Chen, G. X. Dong, Yang Su, Zeyu Li, X. Z. Wu, and Z. X. Li, Role of pairing correlations in the fission process, *Phys. Rev. C* 108, 034306 (2023)
- [47] U. Brosa, S. Grossmann, and A. Müller, Nuclear scission, *Phys. Rep.* 197, 167 (1990).
- [48] S. S. Belyshev, B. S. Ishkhanov, A. A. Kuznetsov, and K. A. Stopani, Mass yield distributions and fission modes in photofission of ^{238}U below 20 MeV, *Phys. Rev. C* 91, 034603(2015).
- [49] D. Pérez-Loureiro, J. Benlliure, J. Díaz-Cortes, J. L. Rodríguez-Sánchez, H. Álvarez-Pol, B. Blank, E. Casarejos, D. Dragosavac, V. Föhr et al., Neutron-rich fragments produced by in-flight fission of ^{238}U , *Phys. Rev. C* 99, 054606(2019).
- [50] O. B. Tarasov and D. Bazin, LISE++: Radioactive beam production with in-flight separators, *Nucl. Instrum. Methods Phys. Res., Sect. B* 266, 4657 (2008).
- [51] M. Caamaño, F. Farget, O. Delaune, K.-H. Schmidt, C. Schmitt, L. Audouin, C.-O. Bacri, J. Benlliure, E. Casarejos et al., Characterization of the scission point from fission-fragment velocities, *Phys. Rev. C* 92, 034606(2015).